International Journal of Thermophysics, Vol. 7, No. 6, 1986

Specific Heats (C_v) of Saturated and Compressed Liquid and Vapor Carbon Dioxide

J. W. Magee[1] and J. F. Ely[1]

Received November 13, 1985

Specific heats of saturated liquid carbon dioxide (C_{sat}) have been measured in the temperature range 220 to 303 K. Specific heats at constant volume (C_v) have been measured at 12 densities ranging from 0.2 to 2.5 times the critical density in the temperature range 233 to 330 K, with pressures varying from 3.4 to 32 MPa. The measurements have been conducted in an adiabatic constant-volume calorimeter of conventional design. Uncertainty of the specific heats is estimated to not exceed 2.0%. Comparisons are made with an extended Benedict–Webb–Rubin equation of state and with the results of other workers.

KEY WORDS: adiabatic calorimetry; carbon dioxide; heat capacity; high pressure; saturated liquid.

1. INTRODUCTION

Thermodynamic properties of a fluid may be calculated from a knowledge of its ideal-gas properties along with an accurate representation of its PVT surface. Specific heats derived in this manner, however, often lack sufficient accuracy since the calculation involves integration of isochoric curvature $(\partial^2 P/\partial T^2)_\rho$. This quantity is known to possess small absolute values except in the vicinity of the critical point and is very difficult to measure accurately. In the case of compressed liquid states ($\rho > 2\rho_c$), additional data are required including the vapor pressure and enthalpy of vaporization or specific heat of the saturated liquid. Direct measurements of specific heats provide useful checks on calculated specific heats when they are available along a path traversing the temperature range of interest.

In this work the specific heats of the saturated liquid (C_{sat}) have been measured over a range of temperatures traversing the entire coexistence

[1] Thermophysics Division, National Bureau of Standards, Boulder, Colorado 80303, U.S.A.

0195-928X/86/1100-1163$05.00/0 © 1986 Plenum Publishing Corporation

840/7/6-4

region, 220 to 303 K. In addition, single-phase specific heats (C_v) have been measured on 12 isochores from 2.0 to 26.0 mol·dm^{-3} with temperatures from 233 to 330 K and pressures up to 32 MPa. It is believed that these data are the most comprehensive specific heats available for the saturated liquid, compressed liquid, and compressed vapor carbon dioxide. Previous specific heat data for carbon dioxide have been summarized in an extensive IUPAC publication [1]. Of the previous investigations, the most comprehensive is due to Amirkhanov et al. [2], who conducted masurements from 276.15 to 403.15 K on densities from 8.81 to 20.79 mol·dm^{-3} in both the single- and the two-phase regions. An overall accuracy of 2 to 4% was assigned to the specific heats. Unfortunately, the range of densities used by Amirkhanov et al. was limited. No dilute vapor or compressed liquid isochores are reported. Also, no saturatd liquid specific heats are reported below 276.15 K. The objective of our investigation is to extend the density range of carbon dioxide specific heat data.

2. APPARATUS AND PROCEDURES

The method by which the specific heat was measured was to observe the temperature rise ΔT when a carefully measured thermal energy Q was supplied to a calorimeter filled with a known amount of substance N. When the heat capacity of the empty calorimeter C_0 is subtracted, the desired specific heat is obtained from

$$C = Q/N\Delta T - C_0/N \tag{1}$$

Thus values for Q, N, and ΔT are required.

The apparatus used in this work is a constant volume adiabatic calorimeter described in detail by Goodwin [3]. Figure 1 illustrates the apparatus. The principal components of the calorimeter are a spherical bomb with a 72-cm^3 (nominal) volume, a fine-diameter (0.015-cm) filling capillary, a guard ring, an adiabatic shield, and a platinum resistance thermometer. The calorimeter bomb is constructed of type 316 stainless steel and has a 5-cm internal diameter and a wall thickness of ca. 0.16 cm. A 100-Ω constantan wire heater is wound on the outer surface of the sphere. The heater wire is varnished onto the surface and surrounded by a lightweight cylindrical copper case which shields the heater from its surroundings and serves also as an anchor for two thermopiles used in heater power control circuits which automatically maintain temperature equality between the bomb and the surrounding guard ring and adiabatic shield. A capsule-type platinum resistance thermometer is encased in a

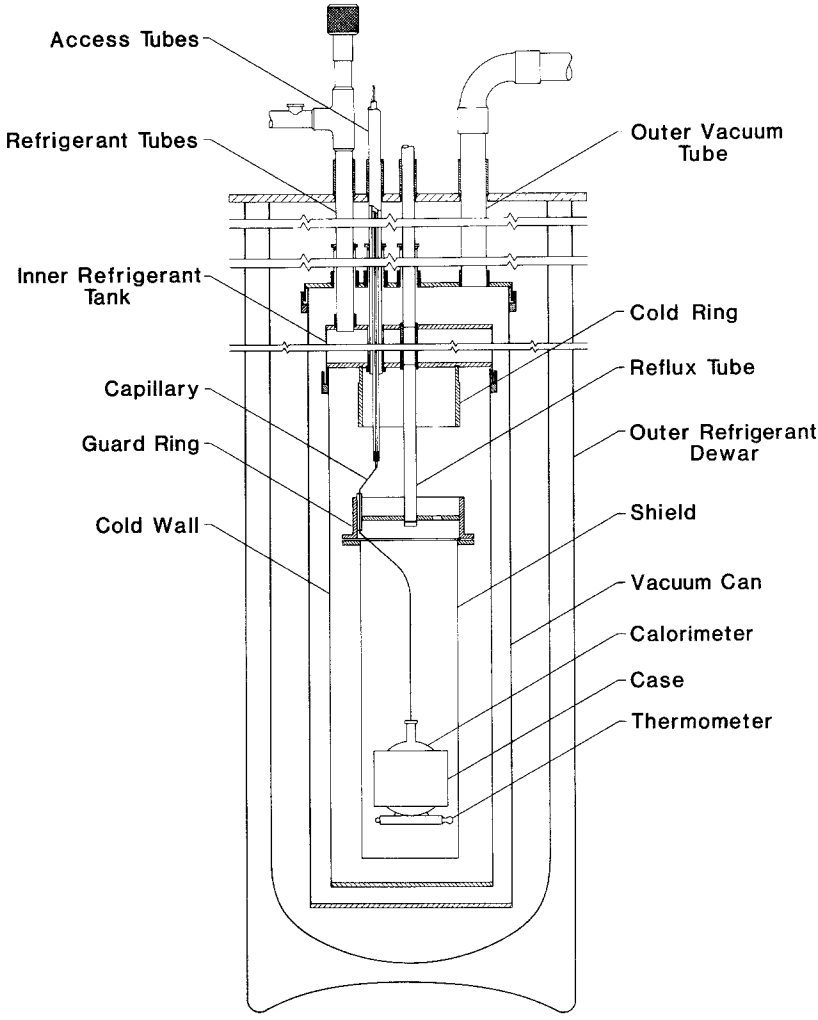

Fig. 1. Principal components of adiabatic calorimeter.

sheath, filled with Woods metal, welded to the bottom of the bomb. The resistance thermometer, calibrated by the NBS Temperature Section on the IPTS-68 scale, has leads attached to a six-dial potentiometer. At the top of an 82-cm capillary is a stainless-steel valve which seals the sample fluid in the calorimeter volume. An electronic counter is used to measure the heating period. A 600-s heating period was used, resulting in a temperature increment ranging from 1 to 12 K, depending on the heater current, which

is variable from 0.05 to 0.15 A. A pair of potentiometers provided for nearly simultaneous readings of the potential and current applied to the heater.

The amount of sample in the calorimeter when the filling valve was sealed could be established by either of two methods. First, as in previous investigations [4, 5], the sample temperature T and pressure P were observed with the valve in the filling capillary cracked open. The amount of sample was obtained from a bomb volume [4] at the filling conditions $V_b(P, T)$ and density $\rho(P, T)$ derived from an equation of state [6]. Second, a gravimetric method was also used. In this procedure, liquified carbon dixide was permitted to drip from a 500-cm^3 aluminum weighing cylinder into the filling capillary until the calorimeter was filled. The filling pressure was fixed by the vapor pressure of liquid carbon dioxide at ambient temperature. The bomb temperature was then adjusted to obtain a desired filling density. When the filling valve had been sealed, the weighing cylinder was inverted and immersed in liquid nitrogen to ensure no mass losses. At a sublimation pressure below 10^{-8} MPa the weighing cylinder valve was tighly closed. The mass of the sample was determined from a weighing of the cylinder and contents prior to and after charging.

After the calorimeter had been filled to the desired density in the single-phase region, the apparatus was cooled to near the triple point. Each measurement sequence commenced in the two-phase region and continued through the coexistence boundary, where a sharp drop in specific heat was observed for each filling. Two-phase specific heats $C_v^{(2)}$ were obtained from primary data after corrections for PV work done by the sample fluid and for vaporization were applied [4]. Values of specific heat of the saturated liquid C_{sat} were derived from $C_v^{(2)}$ measurements for each liquid isochore measured. Measurements of Q and ΔT were continued into the single-phase region until the upper limit of temperature (330 K) or pressure (35 MPa) was obtained. Values of C_v were obtained when adjustments were applied to the primary data for PV work [5] done by the sample. These adjustments were required since the sample holder is a thin stainless-steel sphere which stretches as the pressure increases.

The samples were taken from a cylinder of high-purity carbon dioxide having a mole fraction purity of 0.9999 as certified by the suplier. In-house gas chromatography revealed the presence of trace quantities of light gases—primarily nitrogen and oxygen. The average purity of 14 samples was determined to be 0.999946 mol fraction carbon dioxide.

3. RESULTS AND DISCUSSION

The amount of substance loaded was determined from carbon dioxide's PVT surface at the conditions before the filling capillary valve was sealed or, alternatively, by direct measurement of the sample mass using a gravimetric method. Table I presents each run identification, with all pertinent data on the filling conditions. Runs 900, 1000, and 1100 employed the gravimetric method. All other runs used measurements of the pressure and temperature to obtain density from a 32-term extended Benedict–Webb–Rubin equation of state [6].

3.1. The Specific Heats (C_{sat}) of Saturated Liquid Carbon Dioxide

Specific-heat measurements commenced in the liquid–vapor region at a temperature just above the triple point for each of the 12 isochores. Two-phase specific heats [$C_v^{(2)}$] were measured from ca. 217 K to each isochore's saturation temperature. The experimental values are presented in Table II. Two-phase specific heats were observed to increase with temperature up to the coxistence boundary, where a discontinuous drop to a single-phase value of the specific heat occurred. Table II furnishes details of the primary measurements and adjustments applied to the experimental

Table I. Calorimeter Loading Conditions for the Experimental Runs

Run No.	Pressure (MPa)	Temperature (K)	Density (mol · dm^{-3})	Mass (g)	Calorimeter volume (cm^3)	Total sample (mol)
100	10.794	330.462	8.363		73.558	0.6163
400	12.909	330.646	12.110		73.584	0.8924
500	15.304	333.450	13.960		73.622	1.0291
600	17.532	329.260	16.102		73.635	1.1870
700	9.8197	300.639	18.021		73.443	1.3248
800	10.594	290.417	20.046		73.417	1.4730
900	6.1859	270.008	22.149	71.500	73.298	1.6247
1000	6.2867	251.499	23.951	77.251[a]	73.238	1.7553
1100	6.0724	228.902	25.980	83.705[b]	73.162	1.9020
1200	4.5219	330.202	2.002		73.482	0.1473
1300	9.3170	329.930	6.024		73.538	0.4442
1400	7.5855	330.210	4.113		73.518	0.3035

[a] Mass of discharge, 77.222 g (−0.038% difference).
[b] Mass of discharge, 83.695 g (−0.012% difference).

Table II. The Specific Heat, C_{sat}, of Saturated Liquid Carbon Dioxide

Point No.	P (MPa)	D (mol·dm^{-3})	T (K)	Q (J)	ΔT (K)	C_0 (J·K^{-1})	N (Mol)	$C_v^{(2)}$ (J·mol^{-1}·K^{-1})	C_{sat} (J·mol^{-1}·K^{-1})		Dev. (%)
									Exp.	Eq. (5)	
101	0.7267	26.088	224.696	1356.57	9.578	76.96	0.6163	104.91	—	—	—
102	1.0401	25.263	234.088	1351.15	9.307	77.90	0.6163	109.10	—	—	—
103	1.4314	24.423	243.222	1349.15	9.063	78.77	0.6163	113.67	—	—	—
104	1.9074	23.549	252.114	1348.48	8.819	79.55	0.6163	118.93	—	—	—
105	2.4492	22.659	260.433	1358.38	8.672	80.25	0.6163	123.84	—	—	—
106	3.1085	21.653	268.899	1348.16	8.361	80.92	0.6162	130.19	—	—	—
107	3.8630	20.540	277.094	1351.42	8.127	81.54	0.6162	137.33	—	—	—
108	4.7139	19.265	285.016	1346.99	7.805	82.12	0.6162	146.57	—	—	—
109	5.6593	17.714	292.633	1350.05	7.472	82.65	0.6161	158.82	—	—	—
110	6.6870	15.523	299.839	1352.13	7.026	83.13	0.6159	177.11	—	—	—
401	0.6774	26.238	222.954	1381.30	8.649	76.77	0.8924	92.91	85.49	86.37	1.03
402	0.9438	25.498	231.457	1378.84	8.488	77.65	0.8924	94.99	86.43	86.99	0.65
403	1.2736	24.745	239.790	1377.71	8.312	78.45	0.8924	97.78	88.19	88.56	0.42
404	1.6737	23.964	247.982	1378.23	8.159	79.19	0.8924	100.49	90.07	90.88	0.90
406	2.6856	22.292	263.642	1377.02	7.801	80.51	0.8923	107.50	96.67	97.46	0.82
407	3.3086	21.356	271.203	1364.07	7.560	81.10	0.8923	111.20	101.34	102.24	0.89
408	4.0183	20.311	278.630	1363.58	7.363	81.66	0.8923	115.89	108.54	109.18	0.59
409	4.8119	19.114	285.857	1362.19	7.131	82.18	0.8922	121.82	120.02	120.66	0.53
410	5.7635	17.527	293.410	1366.85	6.812	82.70	0.8922	131.99	145.14	146.46	0.91
411	6.4555	16.109	298.302	627.05	2.988	83.03	0.8913	142.04	183.94	189.09	2.80
412	6.9038	14.871	301.236	625.70	2.874	83.22	0.8913	150.62	248.07	257.66	3.87
413	7.1905	13.663	303.021	157.37	0.696	83.34	0.8913	159.88	395.03	390.85	−1.06
501	0.6501	26.325	221.947	1358.15	7.928	76.66	1.0291	91.95	86.66	86.37	−0.34
503	1.1769	24.952	237.532	1364.79	7.740	78.24	1.0291	95.29	88.76	88.05	−0.80
504	1.5183	24.255	244.993	1361.38	7.598	78.93	1.0291	97.37	90.47	89.95	−0.58

506	2.3960	22.743	259.680	1361.70	7.337	80.19	1.0291	102.36	95.66	95.47	–0.20
507	2.9432	21.900	266.910	1362.85	7.227	80.77	1.0290	104.68	98.95	99.34	0.39
508	3.5602	20.985	273.961	1361.18	7.064	81.31	1.0290	108.14	104.41	104.46	0.05
509	4.3334	19.843	281.618	1358.11	6.861	81.87	1.0290	112.67	113.33	113.11	–0.20
510	5.0947	18.666	288.214	1359.53	6.676	82.34	1.0289	117.73	126.17	126.40	0.18
511	5.9407	17.195	294.706	1355.14	6.389	82.79	1.0288	125.50	151.96	154.25	1.51
523	6.4940	16.017	298.560	346.71	1.593	83.04	1.0287	130.62	185.01	192.87	4.25
524	6.7284	15.408	300.109	346.92	1.557	83.15	1.0280	135.63	213.80	222.67	4.15
525	6.9692	14.644	301.650	347.29	1.563	83.25	1.0280	134.91	260.53	275.88	5.89
601	0.7709	25.959	226.184	1375.99	7.459	77.11	1.1870	90.43	86.67	86.47	–0.23
602	1.0204	25.310	233.563	1375.82	7.367	77.85	1.1870	91.72	87.70	87.30	–0.45
603	1.3203	24.647	240.838	1373.42	7.256	78.55	1.1870	93.26	89.14	88.82	–0.36
604	1.6749	23.962	248.003	1370.19	7.142	79.20	1.1870	94.87	90.87	90.88	0.02
605	2.0881	23.243	255.063	1367.59	7.025	79.80	1.1870	96.72	93.17	93.46	0.31
606	2.5629	22.481	262.004	1368.42	6.927	80.38	1.1869	98.65	96.03	96.61	0.60
607	3.0846	21.688	268.616	1363.89	6.789	80.90	1.1869	101.02	99.97	100.42	0.45
608	3.6856	20.801	275.281	1360.34	6.661	81.41	1.1869	103.38	105.04	105.66	0.59
609	4.3573	19.807	281.838	1364.06	6.531	81.89	1.1869	106.86	113.15	113.44	0.25
610	5.0966	18.663	288.229	1361.31	6.354	82.34	1.1868	111.00	125.66	126.44	0.62
611	5.6723	17.691	292.730	594.41	2.710	82.65	1.1868	115.02	140.86	142.97	1.50
612	6.0465	16.989	295.466	629.59	2.819	82.84	1.1867	118.22	155.87	159.68	2.44
701	0.6783	26.235	222.988	1359.22	6.988	76.78	1.3248	88.85	86.43	86.37	–0.07
702	0.8902	25.634	229.905	1357.49	6.915	77.49	1.3248	89.67	87.17	86.79	–0.43
703	1.1434	25.027	236.716	1350.21	6.792	78.16	1.3248	91.04	88.57	87.88	–0.78
704	1.4424	24.402	243.450	1350.33	6.716	78.79	1.3248	92.27	90.02	89.51	–0.57
705	1.7936	23.748	250.152	1351.85	6.654	79.38	1.3247	93.40	91.60	91.61	0.01
706	2.1948	23.067	256.716	1350.29	6.559	79.94	1.3247	95.01	94.00	94.15	0.16
707	2.6515	22.344	263.192	1349.33	6.462	80.47	1.3247	96.82	97.08	97.22	0.14
708	3.1663	21.567	269.576	1349.01	6.367	80.97	1.3247	98.74	100.97	101.07	0.10
709	3.8023	20.629	276.481	1350.83	6.271	81.50	1.3247	101.00	106.68	106.83	0.14

Table II. *(Continued)*

Point No.	P (MPa)	D (mol·dm^{-3})	T (K)	Q (J)	ΔT (K)	C_0 (J·K^{-1})	N (Mol)	$C_v^{(2)}$ (J·mol^{-1}·K^{-1})	C_{sat} (J·mol^{-1}·K^{-1})		Dev. (%)
									Exp.	Eq. (5)	
710	4.4495	19.668	282.678	1353.29	6.164	81.95	1.3246	103.77	114.63	114.74	0.10
711	4.9665	18.871	287.158	634.47	2.842	82.27	1.3246	106.31	123.25	123.65	0.33
801	0.6538	26.313	222.086	1360.30	6.605	76.68	1.4730	87.75	86.36	86.37	0.01
802	0.8473	25.748	228.611	1353.84	6.522	77.36	1.4730	88.39	87.07	86.66	–0.47
803	1.0779	25.175	235.071	1353.90	6.470	78.00	1.4730	89.09	87.96	87.56	–0.45
804	1.3329	24.622	241.115	1348.68	6.381	78.57	1.4730	90.12	89.31	88.89	–0.47
805	1.6446	24.017	247.438	1351.80	6.337	79.14	1.4730	91.06	90.78	90.70	–0.09
806	2.0028	23.386	253.696	1347.55	6.251	79.69	1.4730	92.21	92.74	92.92	0.19
807	2.4125	22.717	259.916	1341.66	6.159	80.21	1.4730	93.39	95.11	95.58	0.50
808	2.8724	22.007	266.034	1358.36	6.156	80.70	1.4729	94.96	98.41	98.81	0.41
809	3.3897	21.236	272.108	1354.82	6.061	81.17	1.4729	96.58	102.57	102.93	0.35
810	3.7949	20.640	276.405	637.98	2.828	81.49	1.4729	97.75	106.29	106.75	0.44
811	4.0163	20.314	278.611	368.55	1.629	81.65	1.4729	98.08	108.26	109.16	0.83
901	0.6884	26.204	223.349	1358.73	6.263	76.81	1.6247	86.24	85.73	86.37	0.75
902	0.8781	25.666	229.544	1357.35	6.198	77.45	1.6247	87.11	86.82	86.75	–0.08
903	1.1011	25.122	235.661	1344.47	6.102	78.06	1.6246	87.55	87.60	87.67	0.09
904	1.3603	24.566	241.712	1350.19	6.084	78.63	1.6246	88.18	88.70	89.04	0.38
905	1.6598	23.989	247.722	1347.91	6.023	79.17	1.6246	88.99	90.20	90.79	0.66
906	2.0012	23.389	253.669	1346.33	5.962	79.69	1.6246	89.91	92.06	92.91	0.92
907	2.2638	22.955	257.754	629.33	2.774	80.03	1.6246	90.34	93.35	94.60	1.34
908	2.4523	22.654	260.477	628.70	2.757	80.25	1.6246	90.92	94.61	95.85	1.31
1001	0.6108	26.453	220.443	630.57	2.765	76.50	1.7553	86.33	86.34	86.41	0.08
1002	0.6836	26.219	223.178	628.49	2.759	76.80	1.7553	86.01	86.13	86.37	0.28
1003	0.7625	25.983	225.907	628.72	2.756	77.08	1.7553	86.04	86.28	86.46	0.20
1004	0.8476	25.747	228.622	627.06	2.738	77.36	1.7553	86.39	86.77	86.66	-0.13

1005	0.9582	25.462	231.861	632.73	2.756	77.69	1.7553	86.52	87.11	87.04	–0.08
1006	1.0590	25.219	234.583	633.67	2.753	77.95	1.7553	86.70	87.49	87.48	–0.01
1007	1.1672	24.974	237.296	632.38	2.738	78.21	1.7553	87.00	88.02	88.00	–0.02
1008	1.2827	24.726	239.997	631.36	2.726	78.47	1.7553	87.22	88.50	88.61	0.12
1009	1.4057	24.475	242.682	631.10	2.713	78.72	1.7553	87.66	89.23	89.30	0.07
1010	1.5309	24.231	245.242	630.86	2.707	78.95	1.7553	87.76	89.67	90.02	0.39
1101	0.6369	26.367	221.449	635.07	2.667	76.61	1.9020	84.91	85.54	86.38	0.98
1201	0.7700	25.962	226.153	632.33	6.073	77.11	0.1473	183.26	—	—	—
1202	0.9664	25.441	232.091	631.93	5.924	77.71	0.1473	196.48	—	—	—
1203	1.1917	24.920	237.885	633.17	5.796	78.27	0.1473	210.08	—	—	—
1204	1.4465	24.394	243.533	631.04	5.638	78.79	0.1473	224.71	—	—	—
1205	1.7312	23.859	249.037	629.73	5.494	79.29	0.1472	239.63	—	—	—
1206	2.0462	23.313	254.396	628.60	5.351	79.75	0.1472	255.80	—	—	—
1207	2.4383	22.676	260.280	631.92	5.243	80.24	0.1472	273.17	—	—	—
1208	2.8210	22.085	265.387	628.47	5.103	80.65	0.1472	288.19	—	—	—
1301	0.7165	26.119	224.341	1354.34	10.630	76.92	0.4442	113.62	—	—	—
1302	1.0648	25.206	234.732	1351.97	10.283	77.97	0.4442	120.40	—	—	—
1303	1.5074	24.276	244.773	1347.59	9.926	78.91	0.4441	127.92	—	—	—
1304	2.0510	23.305	254.473	1349.70	9.620	79.75	0.4441	136.19	—	—	—
1305	2.7022	22.266	263.859	1348.95	9.290	80.53	0.4441	145.46	—	—	—
1306	3.5708	20.970	274.074	1351.99	8.947	81.32	0.4441	156.92	—	—	—
1307	4.4597	19.653	282.770	1350.97	8.582	81.96	0.4440	169.63	—	—	—
1308	5.4538	18.072	291.066	1346.63	8.151	82.54	0.4439	185.81	—	—	—
1401	0.7932	25.896	226.909	1351.16	11.564	77.19	0.3034	130.60	—	—	—
1402	1.2043	24.893	238.186	1349.17	11.097	78.30	0.3034	142.52	—	—	—
1403	1.7286	23.864	248.990	1344.77	10.628	79.28	0.3034	155.55	—	—	—
1404	2.3755	22.776	259.387	1355.52	10.285	80.16	0.3034	169.94	—	—	—
1405	3.1390	21.607	269.256	1352.54	9.837	80.95	0.3034	186.07	—	—	—
1406	4.0388	20.281	278.830	1351.88	9.409	81.67	0.3033	204.01	—	—	—
1407	4.9766	18.855	287.242	1126.23	7.513	82.27	0.3033	222.47	—	—	—

840/76-5

data. A consistency test was applied to the $C_v^{(2)}$ data via the relation of Yang and Yang [7]. For coexisting phases the relation is

$$C_v^{(2)}/T = -\partial^2 G/\partial T^2 + \rho^{-1}\partial^2 P_{sat}/\partial T^2 \quad (2)$$

where G is the Gibbs free energy per mole and ρ is the average filling density. According to Eq. (2) self-consistent specific-heat data $C_v^{(2)}$ should be represented by a straight line when ploted versus the reciprocal of density along isotherms. Interpolation of $C_v^{(2)}$ measurements to even temperatures was accomplished by fitting the function,

$$C_v^{(2)} = A + BT + CT^2 + DT^3 + ET[T_c - T]^{-0.10} \quad (3)$$

to individual isochores and subsequently calculating interpolated values. Figure 2 demonstrates the linearity of $C_v^{(2)}$ with ρ^{-1} at 230, 240, 250, 260, 270, and 280 K. Values of vapor pressure curvature $\partial^2 P_{sat}/\partial T^2$ were extracted from linear least-squares fits of these isotherms. The results are given in Table III. Also shown in Table III is a comparison between these experimenal results and the values predicted by Ely [8] which derive from published vapor pressures. The two sets of numbers show a remarkably

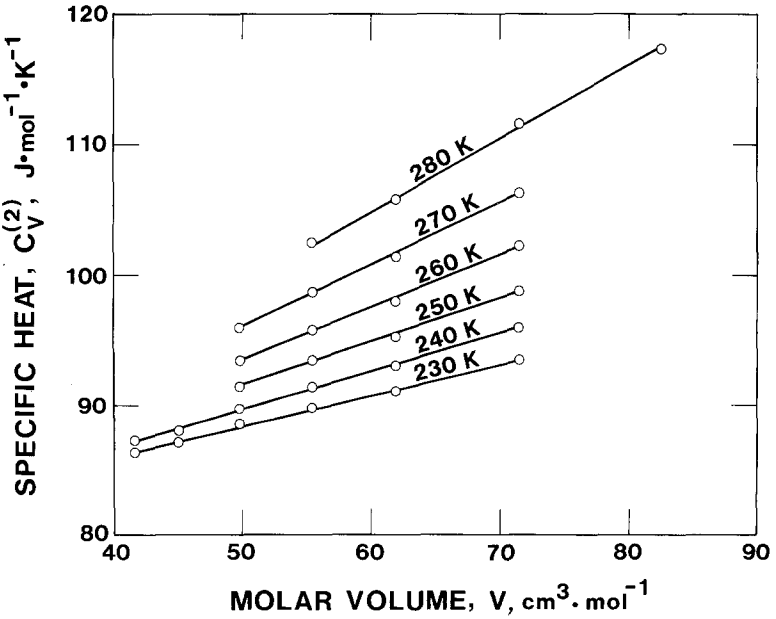

Fig. 2. Variation of two-phase specific heats of carbon dioxide with molar volume.

Table III. Comparison of Vapor Pressure Second Derivative (d^2P_{sat}/dT^2) Derived from Specific-Heat Measurements with a Vapor Pressure Equation [8]

T (K)	d^2P_{sat}/dT^2 (MPa·K^{-2})	
	This work	Ely et al. [8]
230	1.05×10^{-3}	9.54×10^{-4}
240	1.18×10^{-3}	1.13×10^{-3}
250	1.35×10^{-3}	1.31×10^{-3}
260	1.53×10^{-3}	1.51×10^{-3}
270	1.75×10^{-3}	1.73×10^{-3}
280	1.98×10^{-3}	1.98×10^{-3}

good agreement. Deviations diminish with increasing temperature, until at 280 K we observe exact agreement.

An important quantity for thermodynamic calculations of compressed liquid states is the specific heat of the saturated liquid (C_{sat}). At densities greater than critical, our $C_v^{(2)}$ measurements were used to compute values of the specific heat of the saturated liquid via the thermodynamic relationship [9],

$$C_{sat} = C_v^{(2)} - T\rho_{sat}^{-2}(\partial\rho_{sat}/\partial T)(\partial P_{sat}/\partial T) + T[\rho_{sat}^{-1} - \rho^{-1}](\partial^2 P_{sat}/\partial T^2) \quad (4)$$

For eight liquid isochores these values are presented in Table II and are graphed in Fig. 3 versus the saturation temperature. An analytic representation of the temperature dependence of C_{sat} is particularly useful for thermodynamic calculations. Consequently, our specific heats of the saturated liquid have been fit to the equation

$$C_{sat} = C_1 + C_2 T + C_3 T^2 + C_4 T^3 + C_5 T[T_c - T]^{-0.42} \quad (5)$$

where the exponent (-0.42) is the best empirical value for Eq. (5) but has no basis in scaling theory. A weighted linear least-squares routine was employed. Weights were selected which reflect the relative size of the adjustment made to each original $C_v^{(2)}$ datum and are given by

$$\text{Wt} = \text{Abs}[(C_{sat} - C_v^{(2)})/C_v^{(2)}]^{-1} \quad (6)$$

The resulting coefficients of Eq. (5) are given in Table IV. Values calculated at experimental temperatures and their percentage deviations are presented in Table II with the original data. The solid line in Fig. 2 passes through

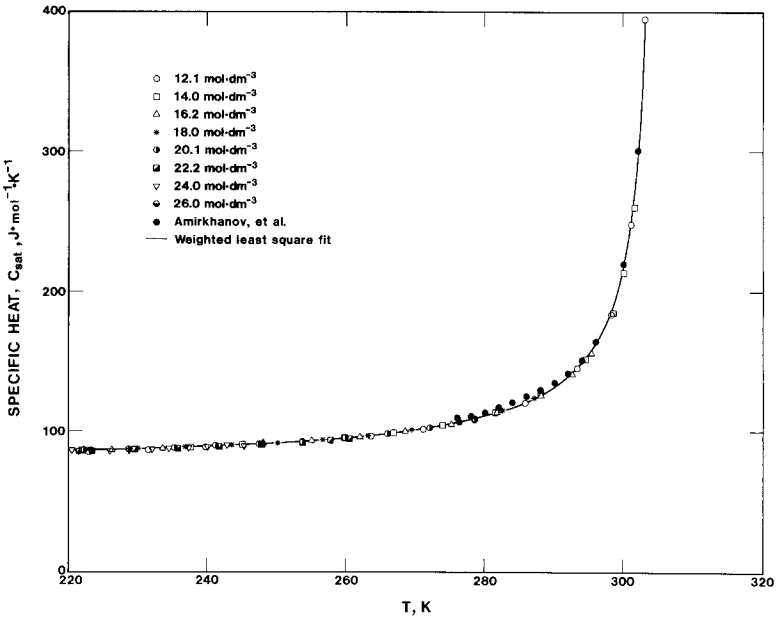

Fig. 3. Saturated liquid specific heats of carbon dioxide. (——) Weighted least square fit; (●) Amirkhanov et al. [2].

values calculated by Eq. (5). The small deviations furnish evidence of the excellent internal consistency of these measurements. The weighted root mean square deviation given by

$$\mathrm{RMS} = 100\left[\sum^{n} (\Delta C_{\mathrm{sat}}/C_{\mathrm{sat}})^2\ \mathrm{Wt} \Big/ \sum^{n} \mathrm{Wt}\right]^{1/2} \tag{7}$$

is 0.24%. Owing to the scarcity of data in the vicinity of the critical point and the higher relative errors of near-critical data, we state the range of reliability of Eq. (5) to be 220 to 300 K.

3.2. The Specific Heats (C_v) of Compressed Vapor and Liquid Carbon Dioxide

Table V presents single-phase specific heats (C_v) for 12 isochores ranging from 2.0 to 26.0 mol · dm^{-3}. They are plotted in Fig. 4. In Table V we furnish the basic calorimetric measurements and adjustments leading to

Table IV. Coefficients C_n for Eq. (5)

Equation[a,b]: $C_{sat} = C_1 + C_2 T + C_3 T^2 + C_4 T^3 + C_5 T(T_c - T)^{-0.42}$
$C_1 = 0.15929 \times 10^4$
$C_2 = -0.18876 \times 10^2$
$C_3 = 0.77482 \times 10^{-1}$
$C_4 = -0.10847 \times 10^{-3}$
$C_5 = 0.14952 \times 10^1$

[a] Critical temperature, $T_c = 304.21$ K [1].
[b] Dimensions of C_{sat}: $J \cdot mol^{-1} \cdot K^{-1}$.

C_v values. A comparison has been made with specific heats calculated from ideal-gas heat capacities and an equation of state via the relation

$$C_v(T, \rho) = C_v^0(T) - T \int_0^\rho (\partial^2 P/\partial T^2)_\rho \, d\rho/\rho^2 \tag{8}$$

A correlation developed by Ely [6, 8] was used in the computations. The integral in Eq. (8) was calculated with a 32-term extended Benedict–Webb–Rubin equation of state. Included in the sources of data used to develop this correlation were spectroscopically derived ideal-gas heat capacities, various sources of PVT data, and the specific heat data of Amirkhanov et al. [2]. Agreement between measured and calculated specific heats is generally acceptable, except in the critical region, where an analytic equation of state cannot be expected to reproduce the nonanalytic behavior observed experimentally. In addition, this correlation fails to give an acceptable agreement with measured specific heats close to the coexistence boundary. A large part of the discrepancy can be assigned to uncertainties in calculating the derivative $(\partial^2 P/\partial T^2)\rho$ from the PVT surface. The discrepancy reduces, as expected, as we depart from the coexistence boundary.

3.3. Comparison with Published Specific Heats

The published specific heat data for carbon dioxide have been critically reviewed by Angus et al. [1]. Of these data, those due to Amirkhanov et al. [2] are perhaps the most comprehensive. Since their isochores are at different densities from those in this work, a direct comparison of C_v measurements is quite difficult if not impossible. However, data which fall on a univariant locus, such as the specific heat of the saturated liquid, furnish a means of comparison. For this purpose, the 324 published $C_v^{(2)}$ data of Amirkhanov et al. were adjusted via Eq. (4) to

Table V. The Specific Heat, C_v, of Carbon Dioxide

Point No.	State conditions			V_{bomb} (cm^3)	Q (J)	ΔT (K)	C_0 ($J \cdot K^{-1}$)	N (mol)	C_v ($J \cdot mol^{-1} \cdot K^{-1}$)		
	P (MPa)	D ($mol \cdot dm^{-3}$)	T (K)						Exp.	Calc., Eq. (8)	Dev. (%)
112	7.6703	8.377	306.469	73.438	366.60	2.964	83.56	0.6152	64.86	50.78	21.70
113	8.0684	8.376	309.467	73.453	368.55	3.086	83.75	0.6152	57.63	49.92	13.37
114	8.4763	8.374	312.555	73.468	367.73	3.131	83.94	0.6152	54.10	49.08	9.28
115	8.8876	8.372	315.689	73.484	367.81	3.169	84.13	0.6152	51.54	48.29	6.32
116	9.3009	8.370	318.853	73.500	368.03	3.196	84.33	0.6152	49.75	47.53	4.46
117	9.7146	8.368	322.039	73.516	367.69	3.215	84.52	0.6152	48.16	46.82	2.79
118	10.1304	8.366	325.257	73.532	367.57	3.222	84.71	0.6152	47.39	46.15	2.62
119	10.5463	8.364	328.493	73.548	367.08	3.229	84.90	0.6151	46.43	45.51	1.98
416	8.3960	12.133	309.087	73.456	147.40	1.114	83.72	0.8912	54.07	49.85	7.81
417	9.0102	12.130	312.055	73.473	630.71	4.849	83.91	0.8912	51.35	49.10	4.38
418	10.0341	12.125	316.976	73.502	628.34	4.925	84.21	0.8912	48.20	47.94	0.54
419	10.8360	12.121	320.808	73.525	349.95	2.766	84.44	0.8912	46.74	47.12	−0.81
420	11.4195	12.118	323.581	73.541	350.10	2.780	84.61	0.8912	45.90	46.56	−1.44
421	12.0076	12.115	326.367	73.558	349.82	2.792	84.77	0.8911	44.99	46.03	−2.30
422	12.5998	12.112	329.164	73.575	350.02	2.802	84.93	0.8911	44.38	45.52	−2.58
423	7.5072	12.137	304.754	73.431	163.73	1.147	83.45	0.8912	66.09	51.03	22.79
424	7.7432	12.136	305.908	73.437	164.02	1.197	83.52	0.8912	59.59	50.70	14.91
425	7.9850	12.135	307.088	73.444	163.57	1.215	83.60	0.8912	56.81	50.38	11.32
426	8.2315	12.134	308.288	73.451	163.76	1.229	83.67	0.8912	55.18	50.06	9.28
513	8.0214	13.997	306.128	73.441	349.50	2.571	83.54	1.0280	50.43	48.20	4.42
514	8.6769	13.994	308.661	73.458	348.86	2.598	83.70	1.0279	48.66	47.67	2.05
515	9.3441	13.990	311.219	73.474	348.77	2.622	83.86	1.0279	47.27	47.15	0.26
516	10.0233	13.987	313.804	73.491	348.79	2.646	84.02	1.0279	45.94	46.65	−1.54
517	10.7114	13.983	316.406	73.508	347.71	2.664	84.18	1.0279	44.52	46.17	−3.71
521	13.5246	13.969	326.893	73.578	347.64	2.677	84.80	1.0278	43.24	44.46	−2.84

522	14.2488	13.966	329.561	73.596	347.61	2.677	84.96	1.0278	43.06	44.08	–2.37
527	8.0167	13.997	306.110	73.441	346.36	2.544	83.54	1.0280	50.63	48.21	4.79
614	7.7589	16.151	302.026	73.424	347.73	2.511	83.27	1.1859	45.81	45.55	0.56
615	8.6257	16.146	304.507	73.443	348.78	2.537	83.43	1.1858	44.83	45.19	–0.80
617	10.3924	16.137	309.507	73.481	348.70	2.558	83.75	1.1858	43.58	44.51	–2.14
618	11.2916	16.133	312.027	73.500	348.49	2.566	83.91	1.1857	43.01	44.19	–2.74
620	13.3079	16.123	317.627	73.543	346.33	2.557	84.25	1.1857	42.38	43.52	–2.68
621	14.2209	16.118	320.142	73.563	345.61	2.554	84.40	1.1857	42.14	43.24	–2.61
623	16.0741	16.109	325.218	73.603	346.03	2.564	84.70	1.1857	41.56	42.72	–2.80
625	17.9472	16.100	330.313	73.643	345.47	2.561	85.00	1.1857	41.23	42.25	–2.46
714	7.4217	18.033	295.447	73.398	360.02	2.548	82.84	1.3236	43.14	43.56	–0.98
715	8.5733	18.027	297.942	73.420	358.75	2.545	83.00	1.3236	42.79	43.34	–1.30
716	9.7347	18.022	300.443	73.442	358.84	2.550	83.17	1.3235	42.48	43.13	–1.53
717	10.6939	18.017	302.499	73.460	359.49	2.558	83.30	1.3235	42.23	42.96	–1.73
718	11.8711	18.011	305.012	73.482	359.32	2.558	83.47	1.3235	42.05	42.76	–1.69
719	13.0541	18.005	307.528	73.505	358.38	2.552	83.62	1.3235	41.88	42.56	–1.63
721	15.4198	17.994	312.533	73.550	359.21	2.563	83.94	1.3234	41.41	42.20	–1.91
722	16.6248	17.988	315.071	73.573	357.86	2.556	84.10	1.3234	41.17	42.03	–2.09
723	17.8330	17.982	317.610	73.597	358.07	2.558	84.25	1.3234	41.02	41.86	–2.06
724	19.0547	17.976	320.172	73.620	359.85	2.570	84.41	1.3234	40.91	41.70	–1.92
725	20.2807	17.970	322.739	73.644	360.06	2.568	84.56	1.3234	40.93	41.55	–1.51
726	21.5104	17.964	325.310	73.668	359.01	2.560	84.71	1.3234	40.82	41.40	–1.42
728	24.0040	17.952	330.517	73.717	358.83	2.554	85.01	1.3234	40.76	41.13	–0.91
814	7.5248	20.062	285.486	73.365	368.41	2.538	82.15	1.4718	41.34	41.94	–1.46
816	11.0629	20.044	291.156	73.425	366.39	2.524	82.55	1.4717	41.13	41.76	–1.52
817	12.6292	20.036	293.658	73.452	366.21	2.526	82.72	1.4717	40.88	41.67	–1.93
819	15.7286	20.021	298.600	73.505	368.04	2.535	83.05	1.4717	40.77	41.51	–1.80
820	17.3113	20.014	301.120	73.532	368.60	2.539	83.21	1.4716	40.64	41.42	–1.93
821	18.8993	20.006	303.648	73.560	370.80	2.557	83.38	1.4716	40.40	41.34	–2.33
822	20.4842	19.998	306.170	73.587	369.82	2.553	83.54	1.4716	40.17	41.26	–2.73
824	23.7641	19.982	311.392	73.645	379.71	2.619	83.87	1.4716	40.00	41.11	–2.78
825	25.3915	19.974	313.984	73.673	377.62	2.598	84.03	1.4716	40.12	41.04	–2.29

Table V. *(Continued)*

Point No.	State conditions			V_{bomb}	Q	ΔT	C_0	N	C_v (J·mol^{-1}·K^{-1})		
	P (MPa)	D (mol·dm^{-3})	T (K)	(cm^3)	(J)	(K)	(J·K^{-1})	(mol)	Exp.	Calc., Eq. (8)	Dev. (%)
826	27.0129	19.967	316.569	73.702	377.81	2.598	84.19	1.4716	40.05	40.97	−2.31
827	28.6316	19.959	319.153	73.730	377.19	2.589	84.34	1.4716	40.11	40.91	−2.01
828	30.2536	19.951	321.745	73.759	378.79	2.595	84.50	1.4715	40.18	40.85	−1.68
912	8.3899	22.139	271.349	73.328	369.13	2.455	81.11	1.6234	40.67	40.95	−0.69
914	11.6936	22.123	275.311	73.378	368.32	2.451	81.41	1.6233	40.46	40.98	−1.29
915	13.6856	22.113	277.704	73.409	367.00	2.436	81.59	1.6233	40.58	40.99	−1.01
916	15.6683	22.103	280.089	73.440	367.90	2.436	81.76	1.6233	40.69	40.99	−0.75
917	16.4512	22.100	281.032	73.452	367.53	2.436	81.83	1.6233	40.55	40.99	−1.10
918	18.4323	22.090	283.421	73.483	367.42	2.430	82.00	1.6232	40.63	40.99	−0.90
919	20.4078	22.081	285.807	73.514	367.42	2.429	82.17	1.6232	40.55	40.99	−1.09
921	24.3235	22.062	290.551	73.576	366.59	2.422	82.50	1.6232	40.37	40.98	−1.51
922	26.2702	22.052	292.916	73.607	365.31	2.408	82.67	1.6232	40.47	40.97	−1.25
923	28.2094	22.043	295.278	73.638	365.95	2.409	82.83	1.6232	40.48	40.96	−1.20
924	30.1473	22.033	297.644	73.669	367.34	2.418	82.98	1.6232	40.37	40.95	−1.45
1013	9.1333	23.936	254.811	73.281	369.62	2.358	79.78	1.7540	41.27	40.62	1.59
1014	11.5725	23.924	257.119	73.315	369.91	2.356	79.98	1.7540	41.35	40.67	1.63
1015	14.0319	23.912	259.454	73.350	369.81	2.354	80.17	1.7539	41.29	40.72	1.39
1016	16.4517	23.900	261.761	73.385	369.08	2.347	80.36	1.7539	41.27	40.76	1.24
1017	18.8529	23.889	264.058	73.420	368.99	2.345	80.54	1.7539	41.21	40.79	1.01
1018	21.2384	23.877	266.348	73.455	367.77	2.334	80.72	1.7539	41.22	40.82	0.96
1019	23.6040	23.866	268.627	73.489	368.11	2.333	80.90	1.7539	41.22	40.85	0.91
1020	25.9650	23.854	270.910	73.524	369.48	2.343	81.08	1.7538	41.06	40.88	0.44
1021	28.3132	23.843	273.188	73.559	368.35	2.332	81.25	1.7538	41.09	40.90	0.46
1105	11.2926	25.953	233.383	73.233	369.01	2.248	77.84	1.9006	42.01	41.57	1.05
1106	14.2855	25.939	235.585	73.272	369.43	2.245	78.05	1.9006	42.14	41.50	1.51

1107	17.2462	25.924	237.777	73.311	367.64	2.232	78.26	1.9005	42.12	41.44	1.61
1108	20.1811	25.910	239.962	73.350	368.34	2.230	78.46	1.9005	42.25	41.38	2.05
1109	23.0928	25.896	242.142	73.390	366.56	2.217	78.67	1.9005	42.22	41.33	2.11
1110	25.9711	25.882	244.308	73.428	366.37	2.212	78.86	1.9005	42.25	41.28	2.31
1111	28.8347	25.868	246.474	73.467	367.28	2.213	79.06	1.9004	42.31	41.24	2.54
1112	31.6816	25.854	248.638	73.506	367.60	2.211	79.25	1.9004	42.35	41.20	2.71
1211	3.3644	2.008	276.757	73.289	367.49	4.208	81.52	0.1472	39.33	36.64	6.83
1212	3.4583	2.008	280.847	73.304	367.04	4.194	81.82	0.1472	38.54	36.29	5.82
1213	3.5507	2.007	284.921	73.318	366.85	4.180	82.11	0.1472	38.23	35.98	5.88
1214	3.6419	2.007	288.986	73.333	367.23	4.172	82.40	0.1472	38.06	35.71	6.18
1215	3.7320	2.006	293.044	73.347	367.35	4.162	82.67	0.1472	37.80	35.46	6.18
1216	3.8289	2.006	297.451	73.363	367.84	4.156	82.97	0.1472	37.45	35.23	5.93
1220	4.1766	2.004	313.630	73.421	365.50	4.089	84.01	0.1471	36.38	34.62	4.82
1221	4.2658	2.004	317.865	73.437	367.49	4.102	84.27	0.1471	35.98	34.52	4.06
1222	4.3508	2.003	321.922	73.451	365.81	4.076	84.51	0.1471	35.41	34.44	2.74
1223	4.4350	2.003	325.970	73.466	365.88	4.066	84.75	0.1471	35.41	34.37	2.93
1311	7.1965	6.034	305.366	73.429	367.61	3.432	83.49	0.4431	53.03	46.84	11.67
1312	7.4976	6.033	308.742	73.444	368.19	3.464	83.70	0.4431	50.69	46.08	9.09
1313	7.7964	6.031	312.129	73.459	367.37	3.477	83.91	0.4430	48.78	45.37	6.99
1314	8.0953	6.030	315.553	73.474	367.61	3.494	84.13	0.4430	47.30	44.70	5.50
1315	8.4000	6.028	319.077	73.490	366.76	3.504	84.34	0.4430	45.59	44.06	3.37
1316	8.6983	6.027	322.562	73.505	366.40	3.505	84.55	0.4430	44.82	43.47	3.02
1317	8.9946	6.026	326.055	73.521	366.40	3.508	84.75	0.4430	44.16	42.93	2.80
1318	9.2895	6.024	329.563	73.537	366.29	3.507	84.96	0.4430	43.69	42.42	2.92
1409	5.8320	4.131	297.004	73.385	366.89	3.780	82.94	0.3032	46.27	42.82	7.46
1411	6.2399	4.120	304.494	73.415	365.98	3.784	83.43	0.3025	43.58	41.58	4.57
1412	6.4431	4.119	308.247	73.430	365.92	3.786	83.67	0.3024	42.64	41.06	3.71
1413	6.6441	4.118	312.008	73.445	366.08	3.786	83.91	0.3024	42.01	40.57	3.42
1415	7.0395	4.116	319.531	73.475	365.28	3.776	84.37	0.3024	40.66	39.72	2.31
1416	7.2344	4.115	323.294	73.490	364.52	3.765	84.59	0.3024	40.19	39.35	2.08
1417	7.4274	4.114	327.059	73.506	364.58	3.758	84.81	0.3024	40.11	39.01	2.73

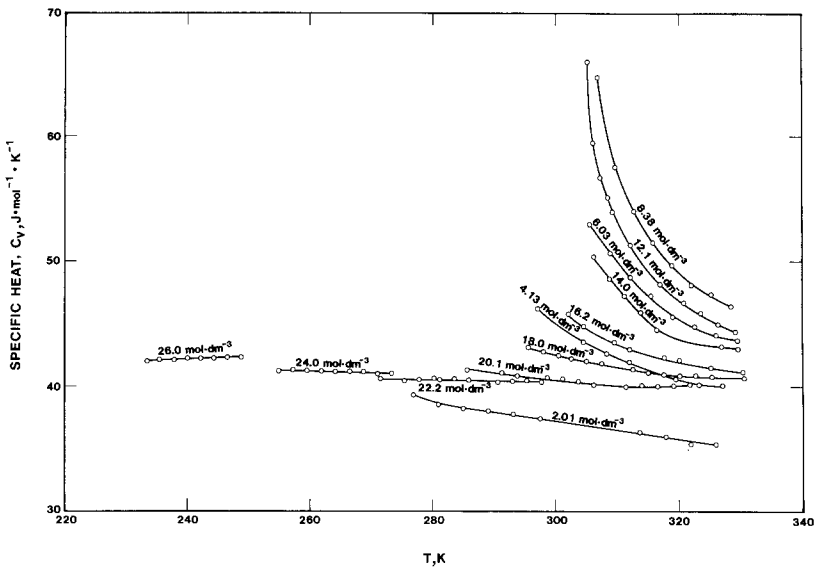

Fig. 4. Single-phase specific heats of carbon dioxide.

obtain values for C_{sat}. Selected values computed in this way are plotted as filled circles in Fig. 3. Although the C_{sat} values derived from Amirkhanov et al. cover a more limited range of temperatures ($276.15\ K \leqslant T \leqslant T_c$), the plot demonstrates that their data deviate substantially from our work. The deviations are strongly biased, as shown. In the temperature range from 276.15 to 300 K, 260 C_{sat} values result in a 1.9% root mean square deviation from Eq. (5). All 260 C_{sat} deviations fell within the 2 to 4% accuracy claimed by Amirkhanov et al.

4. UNCERTAINTIES

Overall accuracy of the specific heat measurement is limited by the uncertainty of ΔT and C_0. The temperature increment ΔT is evaluated at the midpoint of the heating cycle by extrapolating temperature drift rates measured immediately prior to heating and following a 20-min period allowed for thermal equilibration. Its uncertainty ranges from 0.001 to 0.005 K. This uncertainty translates into a 0.1% uncertainty in C_v for a ΔT of 5 K but increases to 0.5% in the vicinity of the critical point, where temperature intervals were of the order of 1 K. The heat capacity of the empty calorimeter C_0 was determined by previous experiments [10] and found to have a precision of about 0.07% and an estimated uncertainty of 0.1%. In our calculations of C_v, the C_0 value must be subtracted from the basic

calorimetric measurement $Q/\Delta T$. When the net is divided by the amount of sample, we are left with the specific heat of the sample. An important consideration is the fraction of the total heat capacity due to the sample. In our single-phase experiments this quantity varied from 49% in the compressed liquid to only 6% in the dilute vapor. The corresponding uncertainty in the specific heat ranges from 0.09 to 1.6% due to the imprecision of C_0.

To a lesser degree, the imprecision in experimental specific heats depends on uncertainties in applied energy Q and amount of sample N. The power supplied to the heater was obtained from nearly simultaneous readings of the potential and current applied to the calorimeter heater. Heater power was observed to be constant to better than 0.01%. A potential source of error in Q is heat leak to or from the sample holder during a heating period. The shield temperature lags behind the sample holder temperature by 0.02 K at the onset of heating. After the power is turned off, the sample temperature lags behind the shield temperature. As observed from chart recordings of the bomb-shield thermopile emf, the area under a $(T_{\text{bomb}} - T_{\text{shield}})$ curve at the beginning of a heating period equals the area under a similar curve following the heating period [10]. The two lags compensate to produce a nearly adiabatic environment over the course of a measurement sequence. Earlier measurements of the thermal resistance between the sample holder and the shield have established that adjustments to the applied energy Q for this effect are negligible in all cases [11]. The time of the heating period was measured by an electronic counter triggered by the potential across the calorimeter heater. The accuracy of the time interval is better than 0.001%, leading to an estimated uncertainty of better than 0.011% in the electrical energy supplied to the calorimeter. The accuracy of the amount of sample in the bomb depends on the method used to load the calorimeter. In one method, the pressure and temperature during filling are measured, the corresponding density is derived from an equation of state, and the moles of sample are evaluated from a calibration of the calorimeter volume. This leads to an uncertainty of 0.1%. For runs 90, 1000, and 1100 a gravimetric method was used to measure the mass loaded into the calorimeter from a weighing cylinder. The mass measurements were conducted on a high-precision balance for which a standard deviation of 0.00051 g was typical. The uncertainty of the gravimetric procedure was obtained by weighing the mass discharged following runs 1000 and 1100. Close agreement was obtained with the mass of sample loaded into the calorimeter. The average error for a single loading is estimated to be 0.01%, a factor of 10 improvement over the other procedure. The cumulative error in the specific heats from all sources is estimated to be lower than 2% in the vapor and 0.5% in the liquid.

ACKNOWLEDGMENTS

The authors would like to express their gratitude to the National Research Council and to the National Bureau of Standards for the NRC-NBS Postdoctoral Fellowship awarded to one of us (JWM) for the support of this research. In addition, the sound advice and encouragement of L. A. Weber and D. E. Diller during all phases of this work are gratefully acknowledged.

REFERENCES

1. S. Angus, B. Armstrong, and K. M. de Reuck, *Carbon Dioxide International Tables of the Fluid State* (Pergamon Press, Oxford, 1976).
2. Kh. I. Amirkhanov, N. G. Polikhronidi, B. G. Alibekov, and R. G. Batyrova, *Teploenergetika* **18**:59 (1971).
3. R. D. Goodwin, *J. Res. Natl. Bur. Stand. (U.S.)* **65C**:231 (1961).
4. R. D. Goodwin and L. A. Weber, *J. Res. Natl. Bur. Stand. (U.S.)* **73A**:1 (1969).
5. R. D. Goodwin and L. A. Weber, *J. Res. Natl. Bur. Stand. (U.S.)* **73A**:15 (1969).
6. J. F. Ely, *Proc. Gas Proc. Assoc. 63rd* (Gas Processors Association, Tulsa, Okla., 1984), pp, 9–22.
7. C. N. Yang and C. P. Yang, *Phys. Rev. Lett.* **13**:303 (1964).
8. J. F. Ely, W. M. Haynes, and J. W. Magee, Natl. Bur. Stand. (U.S.) Monograph, Thermophysical Properties of Carbon Dioxide from 217 to 1000 K at Pressures to 300 MPa (manuscript in preparation) (1985).
9. H. J. Hoge, *J. Res. Natl. Bur. Stand. (U.S.)* **36**:111 (1946).
10. H. M. Roder, *J. Res. Natl. Bur. Stand. (U.S.)* **80A**:739 (1976).
11. B. A. Younglove and D. E. Diller, *Cryogenics* **2**:283 (1962).